

Synthesis, Structure and Physical Properties of Tetrathiafulvalenium Salts of the Ferracarborane Complex *commo*-[3,3'-Fe{1-(C₄H₃S)-1,2-C₂B₉H₁₀}₂]⁻ †

Yaw-Kai Yan,^a D. Michael P. Mingos,^{*,a} Mohamedally Kurmoo,^b Wan-Sheung Li,^c Ian J. Scowen,^c Mary McPartlin,^{*,c} A. Treeve Coomber^d and Richard H. Friend^d

^a Department of Chemistry, Imperial College of Science, Technology and Medicine, South Kensington, London SW7 2AY, UK

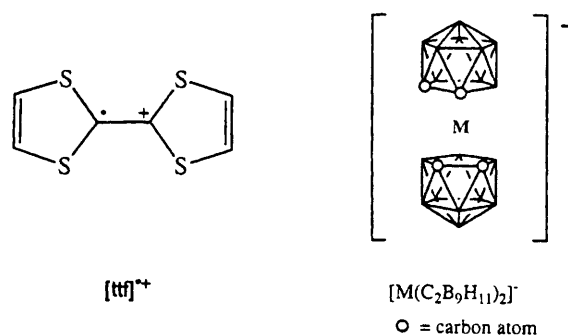
^b The Royal Institution of Great Britain, 21 Albemarle Street, London W1X 4BS, UK

^c School of Applied Chemistry, University of North London, Holloway Road, London N7 8DB, UK

^d Cavendish Laboratory, University of Cambridge, Madingley Road, Cambridge CB3 0HE, UK

The sandwich complex *commo*-[3,3'-Fe{1-(C₄H₃S)-1,2-C₂B₉H₁₀}₂]⁻ **1** and its tetrathiafulvalenium salts [tff]₅[Fe(C₂B₉H₁₀C₄H₃S)₂]₂ **2** and [tff][Fe(C₂B₉H₁₀C₄H₃S)₂] **3** were synthesised in order to study the effect of the thiophene (C₄H₃S) group on the crystal packing, electrical and magnetic properties of ttf–metallacarborane salts. The crystal structure of **2** features unusual two-dimensional networks of ttf units which extend in the *a* and *c* directions. Each ttf sheet contains stacked trimers of ttf units, which propagate along the *a* direction, and bridging ttf units, which lie between the ttf stacks approximately orthogonally to the ttf units within the trimers. The trimers are linked along the *c* direction *via* short S···S contacts (3.56 Å) with these bridging ttf units. In contrast, the crystal structure of compound **3** contains discrete stacked dimers of [tff]⁺ cations. Whilst crystals of **2** are semiconducting ($\sigma_{300\text{K}} = 2 \times 10^{-3} \text{ S cm}^{-1}$) with an activation energy of 0.22 eV, those of **3** are insulating ($\sigma_{290\text{K}} \leq 10^{-7} \text{ S cm}^{-1}$). Both compounds exhibit weak ferromagnetic interactions between the unpaired spins of their [Fe(C₂B₉H₁₀C₄H₃S)₂]⁻ anions, with small positive Weiss constants of 1.9 and 0.5 K respectively.

Although numerous molecular conductors¹ and ferromagnets² have been synthesised, molecular materials containing both magnetic and conducting sublattices are still relatively rare.³ In our studies on charge-transfer salts of paramagnetic metallacarboranes, we have recently reported the salts [tff]⁺[M(C₂B₉H₁₁)₂]⁻ {tff = tetrathiafulvalene [2-(1,3-dithiol-2-ylidene)-1,3-dithiole]; M = Cr, Fe or Ni}⁴. In the chromacarborane salt the [tff]⁺ cations are arranged in sheets with intercationic S···S distances greater than 3.95 Å, whilst in the iron and nickel analogues these cations form discrete stacked dimers. Preliminary conductivity measurements in our laboratory indicated that the chromacarborane salt is a semiconductor ($\sigma_{\text{r.t.}} = 3 \times 10^{-4} \text{ S cm}^{-1}$) with an activation energy of 0.16 eV. On the other hand, the nickelacarborane salt is an insulator, with a room-temperature (r.t.) conductivity of less than 10⁻⁷ S cm⁻¹. Since intermolecular attractive interactions between sulfur atoms are known to exert a strong influence on the packing of molecules in crystals,⁵ it was envisaged that the introduction of thiophene substituents on the metallacarborane anion may enhance the ttf–metallacarborane interaction *via* S···S contacts, thereby suppressing dimerisation of ttf units and encouraging the propagation of mixed-valence ttf stacks. Such an arrangement of ttf units is expected to show a higher electrical conductivity.^{1,6} Alternatively, the thiophene groups may also engage in π – π interactions with the ttf units to produce unusual molecular arrangements, such as interleaved mixed stacks which lie in close proximity to the paramagnetic metal centres. This arrangement may favour



magnetic interactions between the spins on the cations and anions.

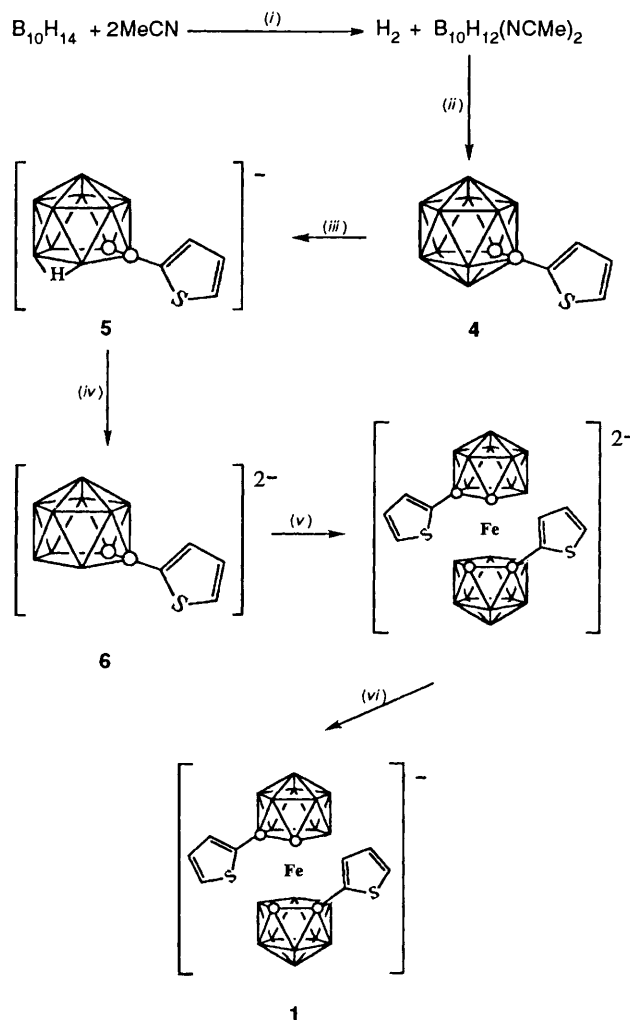
In this paper we report the syntheses of the thiophene-substituted ferracarborane *commo*-[3,3'-Fe{1-(C₄H₃S)-1,2-C₂B₉H₁₀}₂]⁻ **1** and its salts [tff]₅[Fe(C₂B₉H₁₀C₄H₃S)₂]₂ **2** and [tff]⁺[Fe(C₂B₉H₁₀C₄H₃S)₂] **3**. The crystal structures, magnetic properties and electrical conductivities of the ttf salts are also presented.

Results and Discussion

(a) [3,3'-Fe{1-(C₄H₃S)-1,2-C₂B₉H₁₀}₂]⁻ **1**.—(i) *Synthesis*. Well established strategies⁷ were applied to synthesise complex **1**, and the relevant details are summarised in Scheme 1. The yield of 1-(thiophen-2-yl)-1,2-dicarba-*closo*-dodecaborane **4** (52%) is moderate compared to the yields of other 1-substituted carboranes obtained from the alkyne–B₁₀H₁₂(MeCN)₂ reaction (0–90%).^{7,8} A probable competing reaction in this synthesis is the polymerisation of 2-ethynylthiophene. The

† Supplementary data available: see Instructions for Authors, *J. Chem. Soc., Dalton Trans.*, 1995, Issue 1, pp. xxv–xxx.

Non-SI units employed: eV $\approx 1.60 \times 10^{-19} \text{ J}$, $\mu_B \approx 9.27 \times 10^{-24} \text{ J T}^{-1}$.



Scheme 1 Synthesis of complex **1**. (i) MeCN, toluene, heat, 2 h; (ii) 2-ethynylthiophene, toluene, heat, 24 h; (iii) KOH, MeOH, heat, 24 h; (iv) NaH, thf, heat, 3 h; (v) $[\text{FeCl}_2(\text{thf})_2]$, thf, heat, 14 h; (vi) air

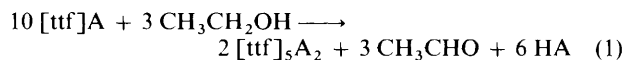
relative ease of this polymerisation was suggested by the observation that freshly prepared, colourless samples of 2-ethynylthiophene turn yellow within an hour at room temperature.

Since the asymmetric *nido*- $[\text{7}-(\text{C}_4\text{H}_3\text{S})\text{-7,8-C}_2\text{B}_9\text{H}_{10}]^{2-}$ **6** is expected to be formed as a racemate, complex **1** should be produced as a mixture of *meso* (DL), DD and LL isomers. However, it has so far proved impossible to resolve the isomeric mixture. In fact, there is yet no evidence for the existence of the *meso* isomer, since only the DD and LL forms were detected in the crystal structures of the ttf salts **2** and **3** (see below).

(ii) *UV/VIS spectrum*. A striking feature of complex **1** is its intense UV/VIS absorption. The Cs^+ and $[\text{NR}_4]^+$ ($\text{R} = \text{Me}$, Et or Bu^n) salts of the complex are all black in the crystalline state and give black-dark brown solutions when dissolved in polar organic solvents. This is in sharp contrast to the analogous complexes $[\text{Fe}(\text{C}_2\text{B}_9\text{H}_9\text{RR}')_2]^-$ ($\text{R} = \text{R}' = \text{H}$ or Me ; $\text{R} = \text{H}$, $\text{R}' = \text{Ph}$), which are all red.⁹ The dark colour of **1** can be attributed to the occurrence of intramolecular charge-transfer transitions between the thiophene group and the iron atom. The electronic spectrum of **1** in dilute acetonitrile solution accordingly shows broad, intense absorption bands between 330 and 450 nm which tail off to as far as ca. 600 nm. These bands are not exhibited by the other ferracarboranes mentioned above. The lowest-energy d-d transition of **1** also occurs at an unusually long wavelength {607 nm, cf. 520 nm for $[\text{Fe}(\text{C}_2\text{B}_9\text{H}_{11})_2]^-$ }.

(iii) *Cyclic voltammetry*. Complex **1** undergoes a quasi-reversible ($\Delta E_p = 110$ mV) one-electron reduction at an $E_{1/2}$ value of -0.34 V [vs. saturated calomel electrode (SCE), 20 °C, 0.1 mmol dm⁻³ MeCN solution with 0.1 mol dm⁻³ $\text{NBu}_4^+\text{PF}_6^-$ supporting electrolyte]. This value, being close to that obtained for $[\text{Fe}(\text{C}_2\text{B}_9\text{H}_{11})_2]^-$ from polarography in 50% aqueous acetone (-0.42 V vs. SCE),⁹ is assigned to the $\text{Fe}^{\text{III}}\text{-Fe}^{\text{II}}$ couple. An anodic peak, attributed to the oxidation of the thiophene ring, occurs at +1.19 V. It is associated with a weaker cathodic peak at +1.09 V ($I_{pa}/I_{pc} \approx 2$). Since the redox potentials of complex **1** are very far from that of the $[\text{tff}]^{+}\text{-tff}$ couple ($E_{1/2} + 0.33$ V vs. SCE in MeCN),¹⁰ the complex is not expected to undergo electron-transfer reactions with either ttf or $[\text{tff}]^{+}$.

(b) $[\text{tff}]_5[\text{Fe}(\text{C}_2\text{B}_9\text{H}_{10}\text{C}_4\text{H}_3\text{S})_2]_2$ **2** and $[\text{tff}]^{+}\text{-}[\text{Fe}(\text{C}_2\text{B}_9\text{H}_{10}\text{C}_4\text{H}_3\text{S})_2]^-$ **3**.—*Synthesis*. Reaction of $[\text{tff}]^{+}\text{-Cl}^-$ with the sodium salt of complex **1** in aqueous solution resulted in the formation of a dark brown powdery precipitate. Rapid concentration of an acetone-ethanol solution of the precipitate under reduced pressure yielded a black microcrystalline material which analysed correctly for $[\text{tff}]^{+}\text{-}[\text{Fe}(\text{C}_2\text{B}_9\text{H}_{10}\text{C}_4\text{H}_3\text{S})_2]^-$ **3**. However, attempts to grow single crystals of the 1:1 salt from the same solvent mixture by slow evaporation yielded black plate-like crystals of the 5:2 salt $[\text{tff}]_5[\text{Fe}(\text{C}_2\text{B}_9\text{H}_{10}\text{C}_4\text{H}_3\text{S})_2]_2$ **2** instead. The stoichiometry of compound **2** suggests a mixed-valence state (between 0 and +1) for the ttf molecules, which is also indicated by the structural and conductivity data of the compound (see below). The most probable source of the neutral/partially oxidised ttf molecules in **2** is the reduction of $[\text{tff}]^{+}$ by ethanol {equation (1) where $\text{A} = [\text{Fe}(\text{C}_2\text{B}_9\text{H}_{10}\text{C}_4\text{H}_3\text{S})_2]^-$ }.



It is noteworthy, however, that slow evaporation of an acetone-ethanol solution containing $[\text{tff}]^{+}\text{-}[\text{Fe}(\text{C}_2\text{B}_9\text{H}_{11})_2]^-$ and half a molar equivalent of ttf yielded only crystals of $[\text{tff}]^{+}\text{-}[\text{Fe}(\text{C}_2\text{B}_9\text{H}_{11})_2]^-$ (identified by its unit-cell parameters⁴). This suggests that the $[\text{Fe}(\text{C}_2\text{B}_9\text{H}_{10}\text{C}_4\text{H}_3\text{S})_2]^-$ anion itself favours the selective crystallisation of the mixed-valence salt **2**.

Single crystals of toluene-solvated complex **3** (black needles) were subsequently grown by layering an acetone-dichloromethane (1:1) solution of **3** with toluene at ca. -20 °C.

(c) *Crystal Structures*.—(i) $[\text{tff}]_5[\text{Fe}(\text{C}_2\text{B}_9\text{H}_{10}\text{C}_4\text{H}_3\text{S})_2]_2$ **2**. The asymmetric unit of compound **2** consists of one ferracarborane anion, one whole ttf unit and three half ttf units. Hence, the unit cell of the compound contains four independent ttf molecules, labelled AB, C, D and E, as shown in Fig. 1. The formula unit contains both D and L isomers of the $[\text{Fe}(\text{C}_2\text{B}_9\text{H}_{10}\text{C}_4\text{H}_3\text{S})_2]^-$ anion, which are related by a crystallographic inversion centre.

The dicarbollide cages of the anion are partially eclipsed in a cisoid configuration with the ligating C_2B_3 faces being rotated by ca. 89° from the position in which the thiophen-2-yl groups are eclipsed. The distance of the iron atom from each C_2B_3 face is 1.56 Å. The C_2B_3 faces are nearly planar [maximum deviations are 0.02 and 0.03 Å, for B(8) and B(8a) respectively] and are inclined by 7.1° to each other. The Fe-C bond lengths [2.115(8)–2.170(9) Å, Table 1] are longer than those observed in the analogous unsubstituted $[\text{Fe}(\text{C}_2\text{B}_9\text{H}_{11})_2]^-$ anion [2.080(3)–2.096(3) Å],⁴ this can be attributed to the steric repulsion between the thiophen-2-yl substituents in **2**. The thiophen-2-yl rings are almost planar [maximum deviations 0.02 Å for C(17) and C(16a) respectively].

The crystal lattice of complex **2** features centrosymmetric stacked trimers of ttf units which propagate along the *a* axis, as shown in Fig. 2. The interplanar separation between the ttf units within a trimer is 3.47 Å, whilst that between adjacent trimers is 3.54 Å. Although the central ttf unit in each trimer (type D) is

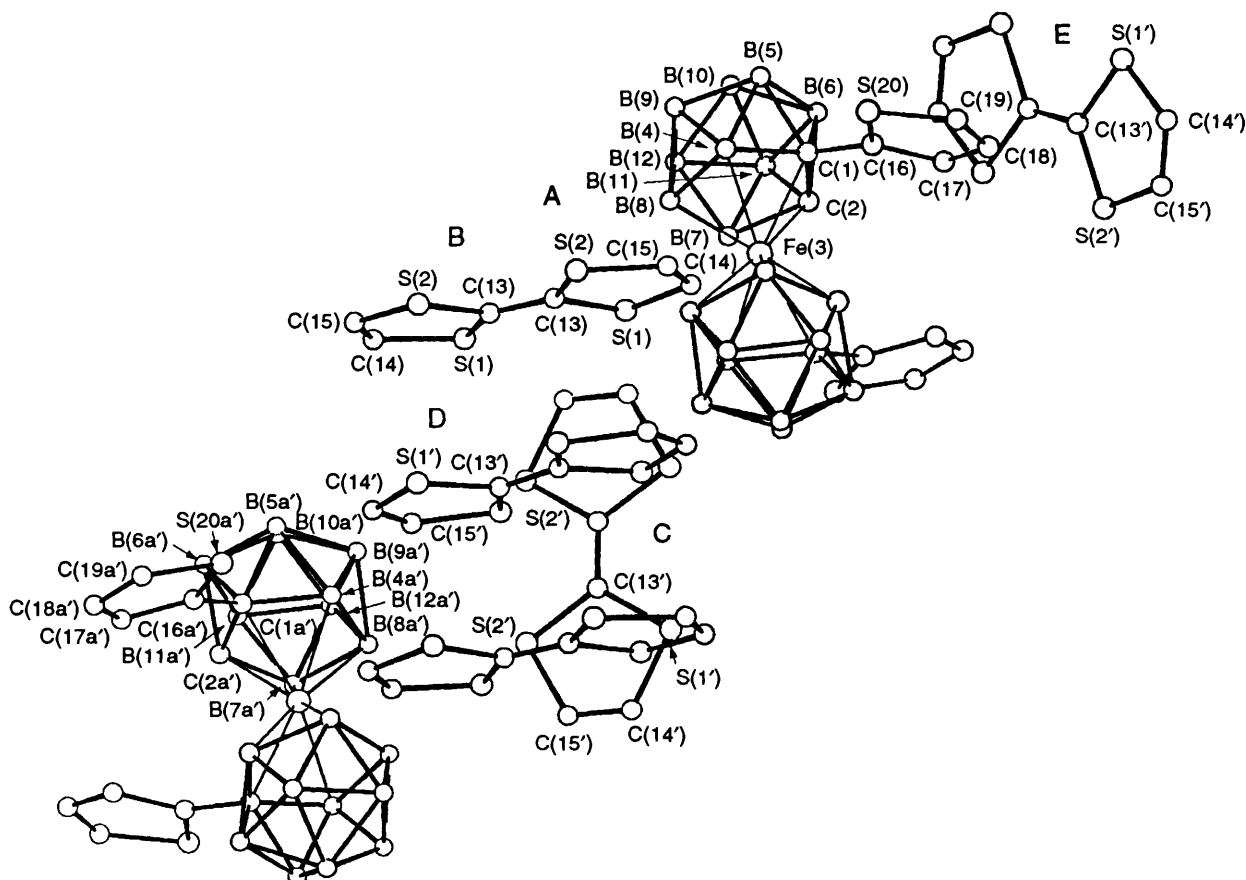


Fig. 1 The formula unit of $[\text{ttf}]_5[\text{Fe}(\text{C}_2\text{B}_9\text{H}_{10}\text{C}_4\text{H}_3\text{S})_2]_2$ **2** showing the labelling adopted for the different types of ttf units (the origin of the unit cell is at the centre of the type D ttf unit)

Table 1 Selected bond lengths (Å) and angles (°) for compound **2**

S(1a)–C(13a)	1.713(9)	Fe(3)–B(4a)	2.172(11)
S(2a)–C(13a)	1.745(11)	Fe(3)–B(7a)	2.109(11)
S(1b)–C(13b)	1.729(11)	Fe(3)–B(8a)	2.149(10)
S(2b)–C(13b)	1.736(9)	C(1)–C(2)	1.593(13)
C(13a)–C(13b)	1.324(13)	C(1)–B(4)	1.683(12)
S(1c)–C(13c)	1.763(8)	C(2)–B(7)	1.696(14)
S(2c)–C(13c)	1.735(10)	B(4)–B(8)	1.773(17)
C(13c)–C(13c')	1.300(15)	B(7)–B(8)	1.762(14)
S(1d)–C(13d)	1.720(8)	C(1a)–C(2a)	1.592(13)
S(2d)–C(13d)	1.686(10)	C(1a)–B(4a)	1.727(13)
C(13d)–C(13d')	1.376(19)	C(2a)–B(7a)	1.673(12)
S(1e)–C(13e)	1.748(12)	B(4a)–B(8a)	1.821(15)
S(2e)–C(13e)	1.746(10)	B(7a)–B(8a)	1.780(16)
C(13e)–C(13e')	1.306(19)	C(1)–C(16)	1.476(13)
Fe(3)–C(1)	2.170(9)	C(1a)–C(16a)	1.468(11)
Fe(3)–C(2)	2.117(8)	C(16)–C(17)	1.428(11)
Fe(3)–B(4)	2.146(10)	C(17)–C(18)	1.407(15)
Fe(3)–B(7)	2.110(11)	C(18)–C(19)	1.310(15)
Fe(3)–B(8)	2.101(10)	C(19)–S(20)	1.675(10)
Fe(3)–C(1a)	2.169(8)	S(20)–C(16)	1.683(10)
Fe(3)–C(2a)	2.115(8)		
C(1)–Fe(3)–C(1a)	124.9(3)	B(7)–Fe(3)–B(8a)	119.4(4)
C(2)–Fe(3)–B(4a)	123.3(4)	B(8)–Fe(3)–B(7a)	119.2(4)
B(4)–Fe(3)–C(2a)	122.7(4)		

rotated by *ca.* 16° with respect to the outer ttf units (type AB), the overlap of the ttf units within each trimer is still best described as 'ring-over-ring'. Adjacent trimers are 'slipped' with respect to one another so that the overlap between adjacent trimers is of the 'ring-over-bond' type. Consequently, the inter-

trimer S...S distances (3.90–3.98 Å) are much longer than the intra-trimer S...S contacts of 3.45–3.54 Å.

The third type of ttf unit (type C) is centrosymmetric and occurs at $(0,0,\frac{1}{2})$, midway between two ttf trimers; it is approximately orthogonal to the ttf units in the trimers. Short S...S contacts of 3.56 Å [S(1c)...S(2d)] link the type C ttf to the centrosymmetrically related type D ttf units on either side, as illustrated in Fig. 2. The continuous two-dimensional layer of linked ttf trimers produced is unprecedented, the only other examples of this type of 'orthogonal' S...S linkage by ttf units occur in $[\text{ttf}]_3[\text{Pt}(\text{S}_2\text{C}_2\text{O}_2)_2]$ and $[\text{ttf}]_2[\text{Ni}(\text{S}_2\text{C}_2\text{H}_2)_2]$, where the linkage is between ttf dimers.^{11,12} For the nickel(II) crystal, electrical conductivity along the bridging direction was established, indicating an appreciable interaction between the dimers and the bridging ttf units. A similar packing motif also occurs in the crystal structure of $[\text{btmttf}]_4[\text{PF}_6]_2$ [btmttf = bis(trimethylene)tetratellurafulvalene], which adopts a layered structure featuring stacked trimers of btmttf units linked *via* short Te...Te contacts with a bridging btmttf unit.¹³

The fourth type of ttf unit (type E) is isolated from the ttf sheets in the crystal, being involved in S...S bonding interactions [S(1e)...S(20) 3.50 Å] with the thiophen-2-yl groups of two adjacent ferracarborane anions related by the inversion centre at $(\frac{1}{2},\frac{1}{2},0)$. These ttf-linked anion pairs propagate along the *a* axis to form a continuous 'ribbon'. Therefore the overall structure consists of layers of these 'ribbons' alternating with the ttf sheets as illustrated in Fig. 3.

In order to estimate the charge distribution amongst the ttf units the bond lengths within these units were examined. A lengthening of the bridging C=C bond and shortening of the C–S bonds involving the bridgehead carbons generally indicate an increase in positive charge on the ttf unit.¹⁴ The C=C bond lengths and average C–S bond lengths of the different ttf units in **2** are given in Table 2, together with some representative

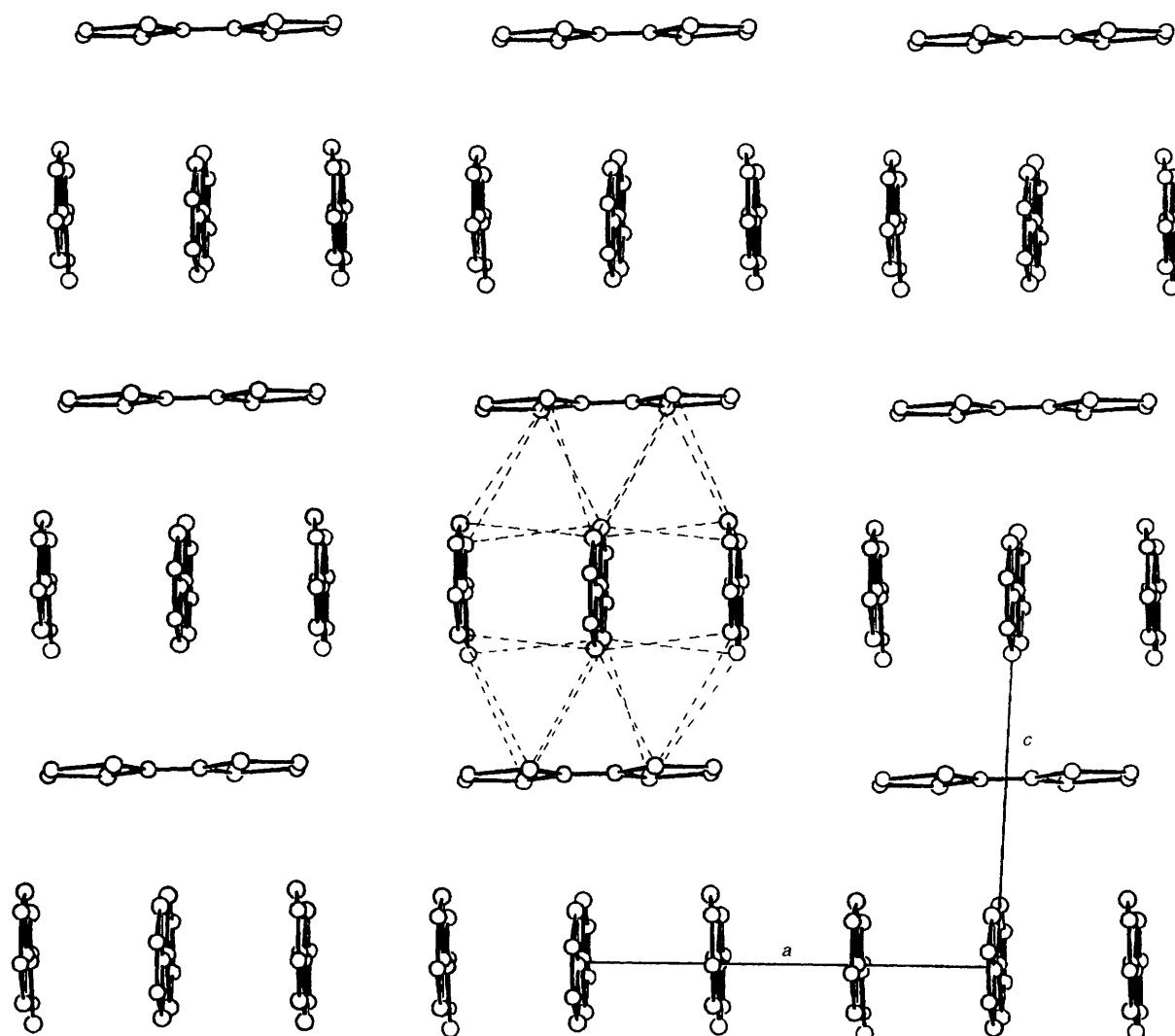


Fig. 2 The two-dimensional sheet of interacting ttf units in the crystal lattice of $[\text{ttf}]_5[\text{Fe}(\text{C}_2\text{B}_9\text{H}_{10}\text{C}_4\text{H}_3\text{S})_2]_2$ **2** viewed down the b axis showing $\text{S}\cdots\text{S}$ contacts of one trimer unit

Table 2 Comparison of C=C and C-S bond lengths (Å) in ttf molecules of different charges

Type	C=C	C-S (mean)	Charge	Ref.
AB	1.324(13)	1.730(10)	+0.5	This work
C	1.300(15)	1.749(9)	0	This work
D	1.376(19)	1.703(9)	+1	This work
E	1.306(19)	1.747(11)	0	This work
ttf	1.349(3)	1.757(2)	0	15
$[\text{ttf}][\text{tcnq}]^*$	1.369(4)	1.743(4)	+0.59	16
$[\text{ttf}][\text{ClO}_4]$	1.404(13)	1.713(9)	+1	17

* tcnq = Tetracyanoquinodimethane.

values of these parameters from the literature. Despite the anomalously short C=C bond lengths in the ttf units of types AB, C and E and the relatively high estimated standard deviations (e.s.d.s) in the bond lengths, it is reasonable to make the charge assignment as given in the Table. Such an assignment is consistent with the stoichiometry of compound **2**. The occurrence of mixed oxidation states in the trimer stacks is also consistent with the semiconducting nature of the compound (see below).

(ii) $[\text{ttf}]^+[\text{Fe}(\text{C}_2\text{B}_9\text{H}_{10}\text{C}_4\text{H}_3\text{S})_2]^- \cdot \text{C}_6\text{H}_5\text{Me}$ **3**. The gross features of the structure (Fig. 4, Table 3) are well established despite poor diffraction from the crystal and disorder in the

Table 3 Selected bond lengths (Å) and angles (°) for compound **3**

S(1a)-C(13a)	1.67(2)	C(1)-B(4)	1.68(3)
S(2a)-C(13a)	1.74(2)	C(2)-B(7)	1.82(3)
C(13a)-C(13b)	1.38(2)	B(4)-B(8)	1.83(3)
S(1b)-C(13b)	1.75(2)	B(7)-B(8)	1.87(3)
S(2b)-C(13b)	1.68(2)	C(1a)-C(2a)	1.65(3)
Fe(3)-C(1)	2.19(2)	C(1a)-B(4a)	1.73(3)
Fe(3)-C(2)	2.16(2)	C(2a)-B(7a)	1.76(3)
Fe(3)-B(4)	2.16(2)	B(4a)-B(8a)	1.86(3)
Fe(3)-B(7)	2.17(3)	B(7a)-B(8a)	1.78(3)
Fe(3)-B(8)	2.18(3)	C(1)-C(16)	1.52(3)
Fe(3)-C(1a)	2.17(2)	C(1a)-C(16a)	1.54(2)
Fe(3)-C(2a)	2.19(2)	C(16a)-C(17a)	1.38(2)
Fe(3)-B(4a)	2.16(2)	C(17a)-C(18a)	1.41(2)
Fe(3)-B(7a)	2.13(2)	C(18a)-C(19a)	1.29(3)
Fe(3)-B(8a)	2.16(2)	C(19a)-S(20a)	1.67(2)
C(1)-C(2)	1.61(3)	S(20a)-C(16a)	1.70(2)
C(1)-Fe(3)-C(1a)	123.2(8)	B(7)-Fe(3)-B(8a)	114.6(9)
C(2)-Fe(3)-B(4a)	117.7(8)	B(8)-Fe(3)-B(7a)	114.1(9)
B(4)-Fe(3)-C(2a)	118.3(8)		

structure, which resulted in high e.s.d.s for all parameters. As in the structure of **2**, only the D and L isomers of the $[\text{Fe}(\text{C}_2\text{B}_9\text{H}_{10}\text{C}_4\text{H}_3\text{S})_2]^-$ anion are present in **3**. The structural features of the anion here are largely similar to those observed

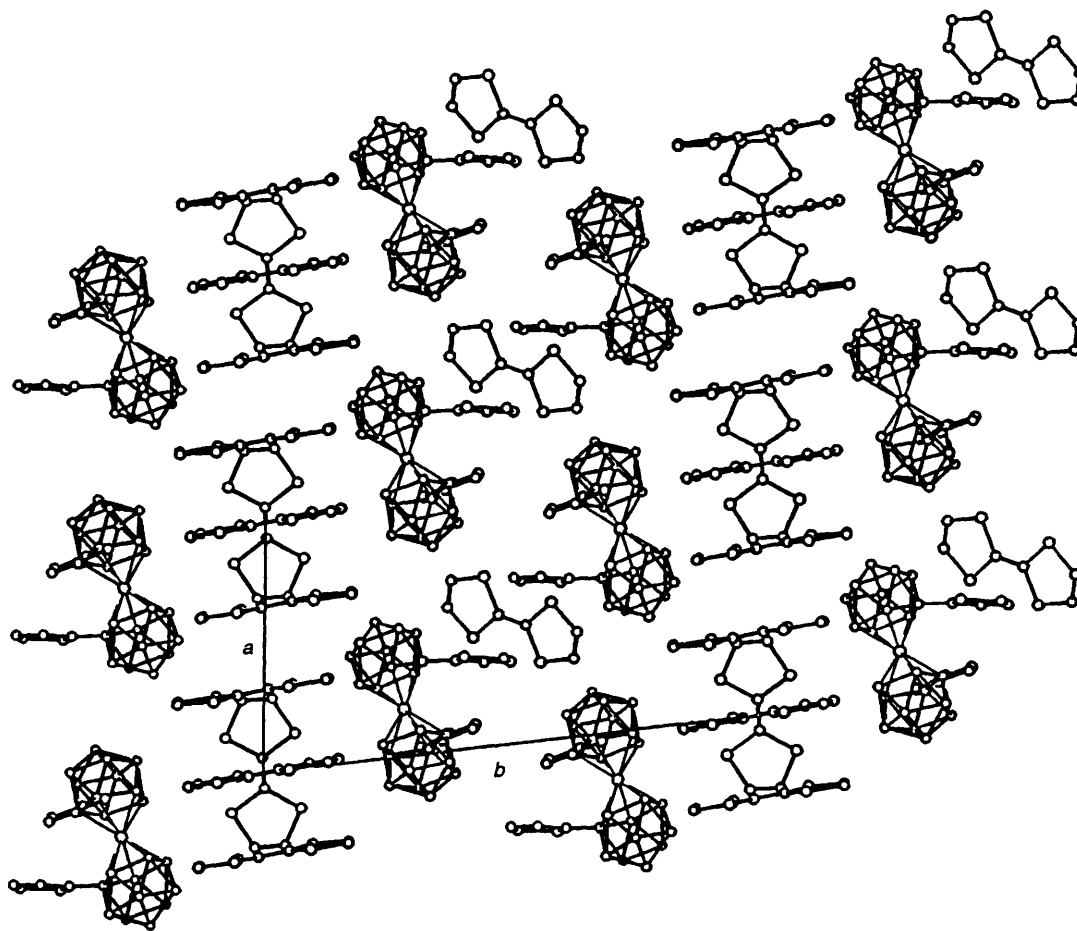
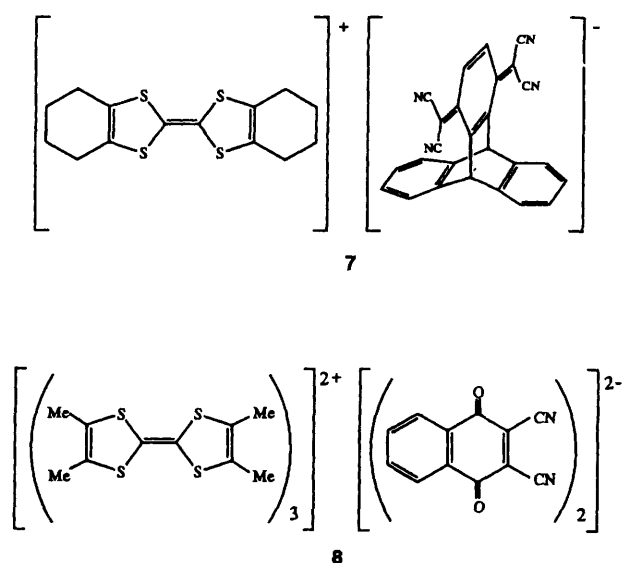


Fig. 3 The crystal packing of $[\text{ttf}]_5[\text{Fe}(\text{C}_2\text{B}_9\text{H}_{10}\text{C}_4\text{H}_3\text{S})_2]_2$ **2**, viewed down the c axis and along the sheets of interacting ttf units, showing the layers of ttf-bridged ferracarborane anions separating the sheets

in **2**. A disorder corresponding to a 180° rotation of one thiophene ring [C(16)–S(20)] about its attachment to the carborane cage, mixing C(17) and S(20) occupancies [S(20'):C(17) and C(17'):S(20) 45:55], was observed. The other thiophene ring is ordered with its sulfur atom, S(20a), oriented *trans* to the unsubstituted cage carbon atom, C(2a). The methyl group of the toluene solvate is disordered over two ring atoms, C(5s) and C(6s).

The $[\text{ttf}]^{2+}$ cations form centrosymmetric stacked dimers in the crystal lattice, as shown in Fig. 4. The $[\text{ttf}]^{2+}$ units in each dimer are virtually eclipsed, with an interplanar separation of 3.45 Å, and feature short intradimer S...S distances of 3.39 and 3.47 Å [for S(1a)...S(2b) and S(1b)...S(2a) respectively]. Each $(\text{ttf}^{2+})_2$ dimer is effectively isolated from other dimers by the surrounding anions and toluene solvate molecules. The toluene molecules are oriented in a face-to-edge manner with respect to the (ttf^{2+}) units, with a relatively short distance of 3.43 Å between S(1b) and the toluene ring centroid. This indicates that there is an electrostatic attraction between the $[\text{ttf}]^{2+}$ cation and the π -electron cloud of the solvate which stabilises their juxtaposition in the crystal lattice. A search of the Cambridge Structural Database¹⁸ revealed only two other compounds with short edge-to-face sulfur...phenyl contacts (sulfur...centroid ≤ 3.5 Å) involving the ttf C_6S_4 group, **7**¹⁹ and **8**.²⁰ The sulfur...centroid distances in these compounds are 3.39 and 3.44 Å respectively.

(d) *Infrared Spectra*.—The infrared spectra of both compounds **2** and **3** (as KBr pellets) exhibit a strong B–H stretching absorption at *ca.* 2560 cm^{-1} , indicating the presence of the metallacarborane component. The presence of dimers of



$[\text{ttf}]^{2+}$ cations in **3** is indicated by the relatively high intensities of the a_g (ν_3) and a_g (ν_6) bands at 1357 and 492 cm^{-1} respectively.²¹ The intensities of these bands are derived from vibronic coupling between the intradimer charge-transfer transition and the otherwise IR-inactive a_g vibrational modes of the $[\text{ttf}]^{2+}$ cations in the dimer.²¹

The IR spectrum of compound **2** is dominated by an intense, broad charge-transfer band which peaks at *ca.* 4120 cm^{-1} and

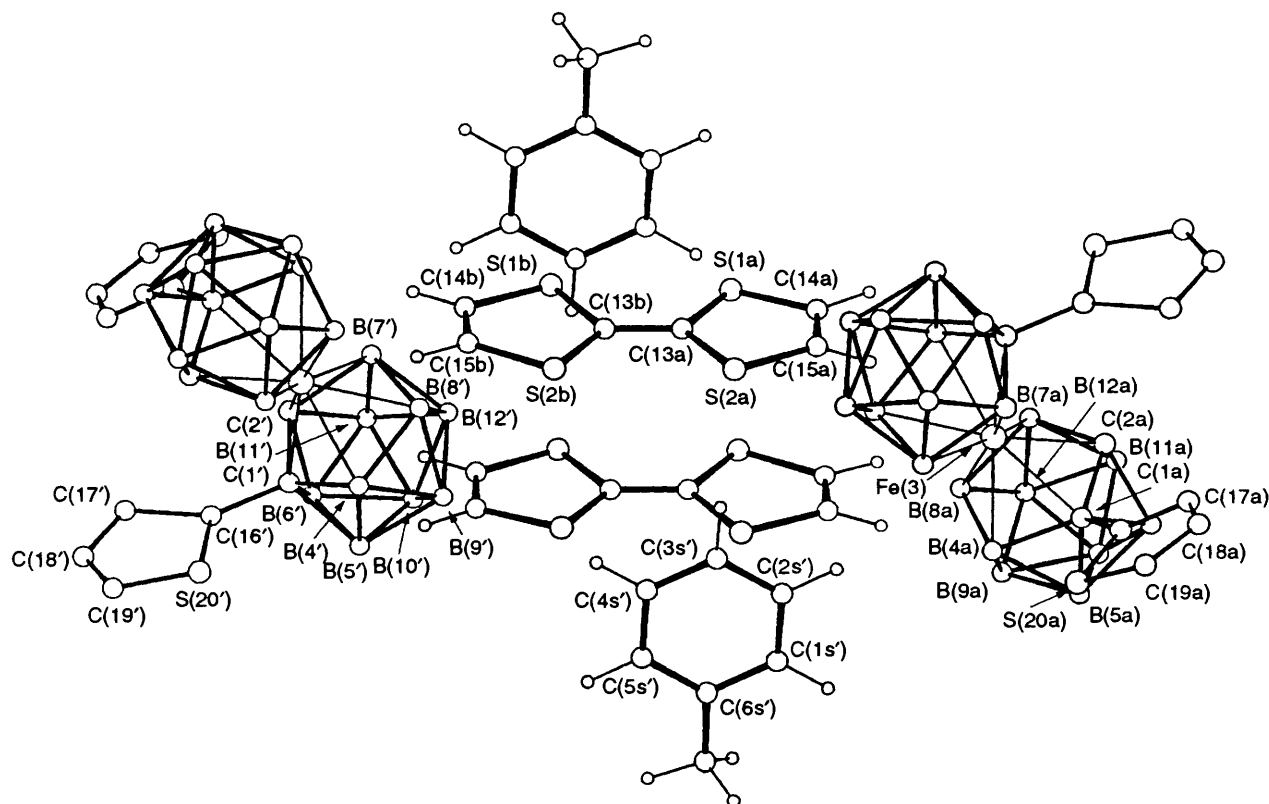


Fig. 4 The centrosymmetric units of $[\text{tff}][\text{Fe}(\text{C}_2\text{B}_9\text{H}_{10}\text{C}_4\text{H}_3\text{S})_2]\cdot\text{C}_6\text{H}_5\text{Me}$ [the disordered methyl group of the toluene solvate is shown attached to C(6s)]

tails off at *ca.* 1410 cm^{-1} . This electronic band (band A in the notation of Torrance *et al.*²²) is characteristic of a mixed-valence state in ttf-type donor molecules. The C–H and B–H stretching absorptions are superimposed on the low-energy side of the charge-transfer band. The $a_g(\nu_3)$ band of **2** occurs between 1400 and 1100 cm^{-1} as a very strong and broad band with its maximum at 1315 cm^{-1} . The $a_g(\nu_6)$ band occurs at 444 cm^{-1} and is also very strong and broad. The unusually high intensity and low frequency of these vibronic bands may indicate that the ttf a_g vibrational modes are strongly coupled to the inter-ttf charge-transfer transitions in **2**.²³

The breadth of the $a_g(\nu_3)$ band and the presence of shoulder peaks on its sides cannot be explained solely by the presence of neutral ttf molecules in the crystal lattice of complex **2** as ttf itself does not absorb strongly in this spectral region.²¹ A more likely explanation is that there are three different types of ttf molecules (A, B and C) lying in close proximity to each other in the lattice, thus facilitating intermolecular charge-transfer and vibronic intensity enhancement of the $a_g(\nu_3)$ modes of all three types of ttf molecules. Different $a_g(\nu_3)$ absorption frequencies are expected for these molecules since they have different charges.²⁴ Correspondingly, the charge-transfer band A presents two broad shoulder peaks on the near-IR side, at 5235 and 6175 cm^{-1} respectively, suggesting the occurrence of more than one charge-transfer transition amongst the three types of ttf molecules.

As in most other mixed-valence ttf salts, the charge-transfer band labelled 'B' by Torrance *et al.*²² is inconspicuous in the spectrum of **2**. It occurs at *ca.* 13 100 cm^{-1} as a relatively weak shoulder.

(e) *Magnetic Properties.*—Between 25 and 295 K the corrected molar magnetic susceptibilities of compounds **2** and **3** (the toluene-solvated crystals) follow the Curie-Weiss law, $\chi = C/(T - \theta)$, with θ values of +1.9 and +0.5 K respectively. The θ values indicate that there is very weak ferromagnetic interaction between the unpaired spins of the ions in both

compounds. In accordance with the presence of spin-paired ttf trimers and dimers in compounds **2** and **3** respectively there is no contribution from the $[\text{tff}]^{+}$ cations to the overall susceptibilities of the compounds. The average moment μ_{av} ($=\sqrt{8C}$) of **2** between 25 and 295 K ($3.0 \mu_B$) indicates the presence of two low-spin iron(III) centres, each having a moment of 2.2 μ_B , per formula unit of the compound [$\mu_{\text{total}}^2 = 2\mu(\text{Fe}^{\text{III}})^2$]. The corresponding value for **3** ($2.0 \mu_B$) is consistent with the presence of one low-spin iron(II) centre per formula unit.

One of the criteria for intermolecular ferromagnetic coupling is that there must be no overlap between the magnetic orbitals of adjacent molecules.²⁵ This condition appears to be satisfied in compounds **2** and **3** since there is no short interanion contact in either compound. On the other hand, the long distances between the iron atoms, on which the magnetic orbitals of the ferracarborane anions are localised, preclude strong spin coupling between the ions (shortest Fe...Fe distances: **2**, 9.88; **3**, 9.28 Å). It is interesting that the compound $[\text{tff}]^{+}[\text{Fe}(\text{C}_2\text{B}_9\text{H}_{11})_2]^{-}$, in which the $[\text{tff}]^{+}$ cations are also dimerised and the Fe...Fe distances are long (shortest Fe...Fe distance 6.34 Å), exhibits weak antiferromagnetic coupling between its anions ($\theta = -2.0$ K).⁴ This suggests that the thiophene groups may be involved in the mechanism of ferromagnetic coupling between the $[\text{Fe}(\text{C}_2\text{B}_9\text{H}_{10}\text{C}_4\text{H}_3\text{S})_2]^{-}$ anions. The possibility of contamination of the samples by ferromagnetic impurities can be discounted on the basis of the results of Honda-Owen analyses,²⁶ which indicate that the levels of such impurities in both compounds **2** and **3** are less than the equivalent of 3 ppm of iron.

(f) *Electrical Conductivity Measurements.*—The electrical conductivities of compounds **2** and **3** were measured on crystals at room temperature. Whilst **2** was found to be semiconducting ($\sigma_{300\text{K}} = 2 \times 10^{-3} \text{ S cm}^{-1}$), **3** was an insulator ($\sigma_{290\text{K}} \leq 10^{-7} \text{ S cm}^{-1}$). Variable-temperature resistance measurements were also performed on compound **2** down to 183 K. A linear plot of $\ln R$ vs. $1/T$ was obtained, giving an activation energy of 0.22 eV.

Conclusion

This study has shown that it is possible to synthesise a semiconducting mixed-valence ttf salt of the $[\text{Fe}(\text{C}_2\text{B}_9\text{H}_{10}\text{C}_4\text{H}_3\text{S})_2]^-$ anion as large single crystals without resort to electrochemical techniques. The $[\text{Fe}(\text{C}_2\text{B}_9\text{H}_{10}\text{C}_4\text{H}_3\text{S})_2]^-$ anion favours the selective crystallisation of a single phase, $[\text{ttf}]_5[\text{Fe}(\text{C}_2\text{B}_9\text{H}_{10}\text{C}_4\text{H}_3\text{S})_2]_2$, from acetone-ethanol solution. The inter-ttf $\text{S}\cdots\text{S}$ interactions are stronger than those between the ttf molecules and the thiophene substituents on the ferracarborane anions. Consequently, the molecular packings in both compounds **2** and **3** are dominated by the formation of clusters of ttf units. This effect is very pronounced in **2**, in which the ttf molecules are interconnected to form two-dimensional networks. Weak ferromagnetic interactions between the $[\text{Fe}(\text{C}_2\text{B}_9\text{H}_{10}\text{C}_4\text{H}_3\text{S})_2]^-$ anions were observed in both compounds **2** and **3**; these interactions appear to occur without the involvement of the ttf units.

Experimental

General.—Tetrathiafulvalene was obtained from Fluka and used as received. Technical grade *nido*-decaborane, $\text{B}_{10}\text{H}_{14}$, a gift from Professor M. L. H. Green (Oxford University) was vacuum-sublimed before use. The compounds $[\text{FeCl}_2(\text{thf})_2]^{27}$ (thf = tetrahydrofuran) and 2-ethynylthiophene²⁸ were made using reported procedures. Organic solvents were of reagent grade, dried by published procedures²⁹ and distilled under N_2 . The solvents were vacuum-degassed before use. Reactions were routinely carried out under N_2 using standard Schlenk techniques.

Physical Measurements.—Infrared spectra in the 5000–220 cm^{-1} region were recorded on a Perkin-Elmer 1720 Fourier-transform spectrometer, UV/VIS spectra using a Perkin-Elmer Lambda 2 spectrophotometer, and near-infrared spectra in the 10 000–3000 cm^{-1} region on a Perkin-Elmer 1760X FT-IR spectrometer. The NMR spectra were recorded either on a JEOL JNM-EX270 FT or a Bruker WM-250 spectrometer; ^1H and $^{11}\text{B}\{-^1\text{H}\}$ chemical shifts were referenced to tetramethylsilane and $\text{BF}_3\cdot\text{OEt}_2$ respectively. Electron-impact (EI) mass spectra were recorded on a VG Micromass 7070B and fast atom bombardment (FAB) mass spectra on a VG AutoSpecQ mass spectrometer using a 3-nitrobenzyl alcohol matrix. Cyclic voltammograms were recorded under N_2 using a platinum-wire working electrode, a silver-wire pseudo-reference electrode and a tungsten-wire auxiliary electrode. The potentials are quoted relative to the saturated calomel electrode using the ferrocene-ferrocenium couple as an external reference.

Magnetic susceptibility measurements were performed in the range 25–295 K using a Faraday balance under magnetic field strengths of 0.76 and 0.87 T. Microcrystalline samples were loaded in quartz buckets having predetermined diamagnetic susceptibilities. The magnetic susceptibilities were corrected for the temperature-independent contribution from the sample by fitting the susceptibility data by the expression $\chi^{-1} = (T - \theta)[C + k(T - \theta)]^{-1}$, where k comprises the diamagnetism of the constituent atomic cores and any temperature-independent paramagnetism of the sample.

Electrical conductivity measurements were carried out on single crystals using the two-probe d.c. method. Contacts were made with platinum paint and 25 μm gold wires.

Syntheses.—*closo*-[1-($\text{C}_4\text{H}_3\text{S}$)-1,2- $\text{C}_2\text{B}_{10}\text{H}_{11}$] **4**. A solution of $\text{B}_{10}\text{H}_{14}$ (3.90 g, 31.9 mmol) in a mixture of acetonitrile (5 cm^3) and toluene (27 cm^3) was refluxed under N_2 for 2 h. A solution of freshly prepared 2-ethynylthiophene (3.59 g, 33.2 mmol) in toluene (4 cm^3) was then added dropwise to the refluxing mixture *via* a pressure-equalised dropping funnel. The resultant brown solution was refluxed for 24 h, after which the solvents were evaporated off under reduced pressure at room temperature. The residue was extracted with CH_2Cl_2 in air and

the extract concentrated under reduced pressure to a volume of ca. 15 cm^3 . On addition of pentane (150 cm^3) to the concentrated extract a dark brown tar separated. The colourless supernatant was collected and the tarry residue redissolved in the minimum volume of CH_2Cl_2 . Pentane was added again and the pentane- CH_2Cl_2 extract collected. This procedure was repeated until a powdery residue was obtained. The pentane- CH_2Cl_2 extracts were combined, filtered and the solvents removed under reduced pressure, leaving a chrome-yellow viscous oil. Crude [1-($\text{C}_4\text{H}_3\text{S}$)-1,2- $\text{C}_2\text{B}_{10}\text{H}_{11}$] **4** was sublimed from the oil at 120–140 $^\circ\text{C}$, ca. 1 mmHg (≈ 133 Pa), and collected on a liquid nitrogen-cooled cold-finger as a pale yellow solid. Recrystallisation from pentane yielded two crops of white flaky crystals (3.74 g, 52%), m.p. 68–70 $^\circ\text{C}$ [Found: C, 31.5; H, 5.9%; M^+ (EI) 226. $\text{C}_6\text{H}_{14}\text{B}_{10}\text{S}$ requires C, 31.8; H, 6.2%; M 226]; $\tilde{\nu}_{\text{max}}/\text{cm}^{-1}$ 3111s (cage CH), 3076s and 3056s (thiophene CH), 2631s, 2599vs and 2564vs (BH), 1429s, 1354m, 1253s, 1222s, 1156m, 1068m, 1068s, 1053m, 1017s, 1001m, 826s, 706vs (br), 570w and 488m (KBr); δ_{H} (250 MHz, CD_2Cl_2) 7.30 [1 H, d, thiophene H(5)], 7.22 [1 H, t, thiophene H(3)], 6.93 [1 H, q, thiophene H(4)] and 3.97 (1 H, br s, cage CH); δ_{B} (80 MHz, CD_2Cl_2) +0.44 (1 B), -2.77 (1 B), -7.77 (4 B), -9.06 (2 B) and -10.48 (2 B).

nido-[7-($\text{C}_4\text{H}_3\text{S}$)-7,8- $\text{C}_2\text{B}_9\text{H}_{11}$] **5**, $[\text{NMe}_3\text{H}]^+$ salt. A solution of potassium hydroxide (3.39 g, 60.4 mmol) in dry methanol (15 cm^3) was added under N_2 to a flask containing compound **4** (3.76 g, 16.6 mmol). The resultant solution was refluxed under N_2 for 24 h, after which the solvent was evaporated off under reduced pressure. The residue was redissolved in ethanol (100 cm^3) and a stream of CO_2 (from 50 g of solid CO_2) was passed through the solution. The precipitated potassium carbonate was filtered off and washed with ice-cold ethanol. The combined filtrate and washing was evaporated to dryness under reduced pressure and the residue redissolved in distilled water. The aqueous solution was filtered through a layer (1 cm) of diatomaceous earth. On treatment of the combined filtrate and washings (total ca. 50 cm^3) with a saturated aqueous solution of $[\text{NMe}_3\text{H}]\text{Cl}$ (5 g, 52.3 mmol) a colourless oil formed. On cooling the mixture to 0 $^\circ\text{C}$ the oil solidified and was filtered off and washed with distilled water. The off-white solid was recrystallised from water (300 cm^3) to give white microcrystals of $[\text{NMe}_3\text{H}][7-(\text{C}_4\text{H}_3\text{S})-7,8-\text{C}_2\text{B}_9\text{H}_{11}]$. A second crop was obtained by evaporating the mother-liquor to 50 cm^3 and slow cooling to 0 $^\circ\text{C}$. The recrystallised product was dried under vacuum and stored under N_2 . Yield: 4.15 g, 91% (Found: C, 39.3; H, 8.7; N, 5.0. $\text{C}_9\text{H}_{24}\text{B}_9\text{NS}$ requires C, 39.2; H, 8.8; N, 5.1%); $\lambda_{\text{max}}/\text{nm}$ (MeCN) 233 ($\epsilon/\text{dm}^3\text{mol}^{-1}\text{cm}^{-1}$ 7400), 245 (sh) (6500) and 268 (7500); $\tilde{\nu}_{\text{max}}/\text{cm}^{-1}$ 3156vs (br) (NH), 3032m (thiophene CH), 2923m, 2962s and 2853m (methyl CH), 2533vs (br) (BH), 1466vs, 1413s, 1384m, 1252w, 1225m, 1175m, 1069m, 1024s, 974vs, 849m, 818m and 694vs (KBr); δ_{H} [270 MHz, $(\text{CD}_3)_2\text{CO}$] 7.76 [1 H, d, thiophene H(5)], 7.55 [1 H, t, thiophene H(3)], 7.48 [1 H, d, thiophene H(4)], 6.82 [1 H, vbr s, NH], 4.02 (9 H, br m, NCH_3), 2.96 (1 H, br s, cage CH) and -1.45 [1 H, vbr s, B(μ -H)B]; δ_{B} [87 MHz, $(\text{CD}_3)_2\text{CO}$] -8.15 (1 B), -9.59 (1 B), -12.47 (1 B), -16.75 (2 B), -17.56 (sh, 1 B), -22.32 (1 B), -32.09 (1 B) and -34.91 (1 B); negative-ion FAB mass spectrum m/z 216 (M^- , 100%).

commo-[3,3'- $\text{Fe}\{1-(\text{C}_4\text{H}_3\text{S})-1,2-\text{C}_2\text{B}_9\text{H}_{10}\}_2]^-$ **1**. A 0.150 g amount of a 60% NaH-mineral oil dispersion (0.090 g NaH, 3.8 mmol) was washed with distilled thf (2 \times 2 cm^3) in a Schlenk tube. Tetrahydrofuran (3 cm^3) was added, followed by a solution of $[\text{NMe}_3\text{H}][\text{nido}\{7-(\text{C}_4\text{H}_3\text{S})-7,8-\text{C}_2\text{B}_9\text{H}_{11}\}]$ (0.280 g, 1.02 mmol) in thf (7 cm^3) at room temperature. The mixture was stirred at room temperature until the initial vigorous evolution of hydrogen ceased (ca. 15 min); it was then refluxed under N_2 for 3 h. (The nitrogen flow rate was increased for ca. 30 min after 90 min of refluxing so as to remove the NMe_3 generated in the reaction and to halve the solvent volume.) After cooling to room temperature and allowing the excess of

NaH to settle, the supernatant was transferred *via* a steel cannula to a stirred suspension of $[\text{FeCl}_2(\text{thf})_2]$ (0.275 g, 1.01 mmol) in thf (3 cm³). The NaH residue was washed with distilled thf (3 cm³) and the washing was added to the reaction mixture. The deep purple reaction mixture was concentrated under reduced pressure to a volume of *ca.* 4 cm³ and then refluxed under N₂ for 14 h. The solvent was removed and the residue extracted with a mixture of diethyl ether (20 cm³) and 1 mol dm⁻³ hydrochloric acid (2 cm³). The ether phase was isolated and evaporated to dryness. The residue was extracted into a minimum volume of distilled water, giving a dark green solution which was treated with a concentrated aqueous solution of $[\text{NMe}_4]\text{Cl}$ (0.16 g, 1.5 mmol). The dark green fine powdery precipitate formed was collected on a glass frit (No. 3) and washed with distilled water. It was then dissolved in acetone (10 cm³) to give a very dark brown solution. Distilled water (10 cm³) was added and the resultant solution concentrated very slowly under reduced pressure in a warm water-bath (*ca.* 60 °C) until it became light greenish brown. The mixture was cooled to room temperature under N₂ and the black microcrystalline precipitate of $[\text{NMe}_4][\text{commo-3,3'}\text{-Fe}\{1\text{-(C}_4\text{H}_3\text{S)}\text{-1,2-C}_2\text{B}_9\text{-H}_{10}\}_2]$ was collected by suction filtration. Yield: 0.121 g, 44% (Found: C, 34.5; H, 6.30; N, 2.4. C₁₆H₃₈B₁₈FeNS₂ requires C, 34.4; H, 6.85; N, 2.5%). The anion **1** can also be precipitated as the Cs⁺, $[\text{NEt}_4]^+$ or $[\text{NBu}_4]^+$ salts. Whilst the Cs⁺ and $[\text{NEt}_4]^+$ salts could be effectively recrystallised from aqueous acetone as described above, the $[\text{NBu}_4]^+$ salt gave an oil under these conditions. A mixture of CH₂Cl₂ and hexane was found to be the best solvent mixture for recrystallising the $[\text{NBu}_4]^+$ salt. $\lambda_{\text{max}}/\text{nm}$ ($[\text{NMe}_4]^+$ salt, MeCN) 244 ($\epsilon/\text{dm}^3 \text{ mol}^{-1} \text{ cm}^{-1}$ 25 000), 277 (18 000), 330 (infl) (8600), 395 (infl) (3500), 486 (sh) (930), 540 (infl) (760) and 607 (sh) (610); $\tilde{\nu}_{\text{max}}/\text{cm}^{-1}$ (Cs⁺ salt) 3105w (cage CH), 3076w and 3026w (thiophene CH), 2550vs (br) (BH), 1428w, 1352w, 1242w, 1163w, 1073m, 1035m, 993s, 834m, 716s, 694s and 356m (KBr); negative ion FAB mass spectrum m/z 485 (M^- , 100%).

$[\text{tff}]^+\text{Cl}^-$. Concentrated hydrochloric acid (12 mol dm⁻³, 0.10 cm³, 1.2 mmol HCl) was added dropwise to a magnetically stirred solution of ttf (0.25 g, 1.2 mmol) in acetonitrile (45 cm³) at room temperature. A 0.4 cm³ amount of 6% aqueous H₂O₂ (0.024 g H₂O₂, 0.7 mmol) was then added dropwise to the stirred mixture. The mixture turned deep purple immediately and a dark brown fine precipitate was formed. The mixture was stirred for 30 min at room temperature and then kept at *ca.* -10 °C for 90 min. The precipitate was filtered off, washed with acetone (8 cm³) and dried under vacuum. The crude product was then stirred with dried, distilled acetonitrile (15 cm³) in a 90 °C water-bath for 20 min. The mixture was cooled to room temperature and then left at -10 °C for 30 min. The black microcrystals of $[\text{tff}]^+\text{Cl}^-$ so formed were filtered off and dried under vacuum. Yield: 0.258 g, 88% (Found: C, 29.65; H, 1.8. Calc. for C₆H₄ClS₄: C, 30.05; H, 1.7%).

$[\text{tff}]^+[\text{Fe}(\text{C}_2\text{B}_9\text{H}_{10}\text{C}_4\text{H}_3\text{S})_2]^-$ **3**. A solution of $[\text{NMe}_4][\text{commo-3,3'}\text{-Fe}\{1\text{-(C}_4\text{H}_3\text{S)}\text{-1,2-C}_2\text{B}_9\text{H}_{10}\}_2]$ (0.103 g, 0.18 mmol) in acetone was loaded on to a column (2 × 32 cm) of Dowex 50 cation-exchange resin (Na⁺ form) and eluted with acetone. The acetone was evaporated off from the aliquot containing the Na⁺ salt of **1** under reduced pressure and the residue redissolved in distilled water (*ca.* 10 cm³). Slow addition of a filtered aqueous solution (*ca.* 60 cm³) of $[\text{tff}]^+\text{Cl}^-$ (0.066 g, 0.28 mmol) to the magnetically stirred solution of the Na⁺ salt of **1** at room temperature resulted in the formation of a brown colloidal suspension. Sufficient solid potassium bromide was added to the stirred suspension to cause flocculation. The mixture was then filtered through a glass frit (No. 3) and the collected brown solid was washed with distilled water. The solid was dissolved in the minimum volume of acetone, a three-fold amount of ethanol was added and the solution was concentrated under reduced pressure at *ca.* 40 °C to a volume of *ca.* 3 cm³. The mixture was left at -10 °C overnight and then filtered to give 0.052 g (42% yield) of compound **3** as black

Table 4 Crystal and refinement data for compounds **2** and **3**

Compound	2	3
Chemical formula	C ₅₄ H ₇₂ B ₃₆ Fe ₂ S ₂₄	C ₂₅ H ₃₈ B ₁₈ FeS ₆
<i>M</i>	1991.5	781.3
Crystal system	Triclinic	Monoclinic
Space group	<i>P</i> $\bar{1}$ (no. 2)	<i>P</i> 2 ₁ / <i>c</i> (no. 14)
<i>a</i> /Å	10.666(3)	10.198(2)
<i>b</i> /Å	21.429(6)	32.301(5)
<i>c</i> /Å	9.884(3)	12.160(3)
α /°	102.81(5)	90
β /°	93.76(4)	109.51(2)
γ /°	82.01(4)	90
<i>U</i> /Å ³	2180.0(16)	3775.6(18)
<i>D_c</i> /g cm ⁻³	1.517	1.375
<i>Z</i>	1	4
<i>F</i> (000)	1012	1600
μ (Mo-K α)/cm ⁻¹	9.1	7.3

microcrystals (Found: C, 31.7; H, 4.0. C₁₈H₃₀B₁₈FeS₆ requires C, 31.4; H, 4.4%). Layering an acetone-CH₂Cl₂ (1 : 1) solution of **3** with toluene at -20 °C afforded toluene-solvated crystals of **3** (Found: C, 38.4; H, 4.8. C₂₅H₃₈B₁₈FeS₆ requires C, 38.4; H, 4.9%; $\tilde{\nu}_{\text{max}}/\text{cm}^{-1}$ 3078s (br), 2560vs (br), 1494w, 1474m, 1430w, 1357vs, 1260m, 1076m, 1031m, 991s, 830m, 741m, 697s, 690s, 492m, 465w and 355w (KBr).

$[\text{tff}]_5[\text{Fe}(\text{C}_2\text{B}_9\text{H}_{10}\text{C}_4\text{H}_3\text{S})_2]_2$ **2**. Non-solvated complex **3** (0.030 g, 0.054 mmol) was dissolved in acetone (*ca.* 10 cm³) in a Schlenk tube. An equal volume of ethanol was added and the solution concentrated under reduced pressure at room temperature until a trace amount of precipitate was formed. It was then left to evaporate through a needle-punctured rubber septum at room temperature under a slow stream of N₂ for 2 weeks, during which time a very small amount of fine black precipitate was formed. The solution was filtered under N₂ and concentrated under reduced pressure at room temperature until a thick black liquid remained. The liquid was left undisturbed under N₂ at room temperature for 1 week, after which it was diluted with methanol (*ca.* 1 cm³). The solution was decanted off and the black plate-like crystals of compound **2** that remained were washed with another 1 cm³ of methanol and dried under vacuum (yield: 0.014 g, 65%) (Found: C, 32.8; H, 3.4. C₅₄H₇₂B₃₆Fe₂S₂₄ requires C, 32.6; H, 3.6%; $\tilde{\nu}_{\text{max}}/\text{cm}^{-1}$ 3068m, 2554vs (br), 1474w, 1347vs (sh), 1315vs (vbr), 1256vs, 1200m (sh), 1170m (sh), 1095m, 1033w, 990m, 823w, 793w, 781vw, 731s, 694m, 658m and 444s (br) (KBr).

X-Ray Crystallography.—The crystal data for compounds **2** and **3** are summarised in Table 4. (i) *Data collection*. A black plate of compound **2** (dimensions 0.48 × 0.40 × 0.02 mm) and a brown-black plate of **3** (0.31 × 0.21 × 0.10 mm) were mounted on quartz fibres and data were collected with a Philips PW1100 diffractometer using graphite-monochromated Mo-K α radiation ($\lambda = 0.71069$ Å) by the method described previously.³⁰ The crystal of **3** diffracted rather poorly and therefore data were collected in the limited range θ 3–21°; data for **2** were collected in the range θ 3–25°. Scan widths of 0.90 and 0.80° were used for **2** and **3** respectively and a scan speed of 0.05° s⁻¹ in each case. Three reference reflections measured at 5 h intervals showed no significant changes in intensity in either case. Of 4176 reflections measured for **2**, 3127 were unique with $I/\sigma(I) > 3$ ($R_{\text{int}} = 0.040$). For **3**, 1746 reflections were measured, of which 1403 were unique with $I/\sigma(I) > 3$ ($R_{\text{int}} = 0.059$).

(ii) *Structure solution and refinement*.³¹ $[\text{tff}]_5[\text{Fe}(\text{C}_2\text{B}_9\text{H}_{10}\text{C}_4\text{H}_3\text{S})_2]_2$ **2**. The positions of all non-hydrogen atoms were obtained from direct methods. A series of Fourier-difference-syntheses using low-angle data ($\sin \theta < 0.35$) revealed the positions of all the hydrogen atoms of the structure; they were included in structure-factor calculations with fixed thermal

Table 5 Fractional atomic coordinates for complex 2

Atom	x	y	z	Atom	x	y	z
S(20)	0.372 1(3)	0.402 8(1)	-0.592 6(3)	C(2a)	0.068 1(8)	0.367 4(4)	-0.459 5(9)
S(20a)	0.029 4(3)	0.316 3(2)	-0.077 4(3)	B(4a)	0.009 5(10)	0.253 9(5)	-0.416 1(11)
S(1a)	0.341 5(3)	0.056 5(1)	0.168 7(3)	B(5a)	-0.127 2(11)	0.313 1(6)	-0.394 9(12)
S(2a)	0.332 5(3)	0.049 0(1)	-0.128 0(3)	B(6a)	-0.087 9(10)	0.385 9(5)	-0.419 9(11)
S(1b)	0.326 2(3)	-0.096 7(1)	0.113 5(3)	B(7a)	0.096 8(10)	0.317 1(5)	-0.613 0(11)
S(2b)	0.307 0(3)	-0.101 4(1)	-0.183 0(3)	B(8a)	0.054 5(10)	0.241 9(5)	-0.595 5(11)
S(1c)	0.158 0(3)	-0.077 4(1)	0.478 0(3)	B(9a)	-0.106 3(11)	0.256 4(6)	-0.552 9(12)
S(2c)	0.144 5(3)	0.062 8(1)	0.510 0(3)	B(10a)	-0.168 7(11)	0.336 9(5)	-0.553 9(12)
S(1d)	0.016 8(2)	0.092 9(1)	0.134 6(3)	B(11a)	-0.040 7(10)	0.374 4(5)	-0.587 8(11)
S(2d)	0.000 6(3)	0.051 2(1)	-0.163 1(3)	B(12a)	-0.055 7(11)	0.294 8(5)	-0.672 7(11)
S(1e)	0.445 5(3)	0.421 6(2)	0.080 1(4)	C(16a)	0.045 8(8)	0.359 7(4)	-0.198 1(9)
S(2e)	0.685 6(3)	0.441 9(2)	-0.017 3(4)	C(17a)	0.081 4(8)	0.420 6(4)	-0.132 8(10)
Fe(3)	0.191 57(11)	0.282 74(6)	-0.444 63(12)	C(18a)	0.095 9(11)	0.425 4(6)	0.013 8(12)
C(1)	0.374 3(8)	0.318 3(4)	-0.419 6(8)	C(19a)	0.069 7(11)	0.375 5(6)	0.056 1(12)
C(2)	0.329 4(8)	0.302 2(4)	-0.282 0(8)	C(13a)	0.331 6(8)	0.008 2(4)	0.006 3(9)
B(4)	0.365 2(10)	0.254 8(5)	-0.553 3(11)	C(14a)	0.347 7(10)	0.126 7(5)	0.112 6(11)
B(5)	0.513 2(11)	0.270 1(5)	-0.469 1(11)	C(15a)	0.345 1(10)	0.122 3(5)	-0.019 4(11)
B(6)	0.488 9(10)	0.303 3(5)	-0.292 0(11)	C(13b)	0.321 9(8)	-0.054 3(4)	-0.016 9(9)
B(7)	0.284 4(10)	0.202 6(5)	-0.306 5(10)	C(14b)	0.320 8(10)	-0.172 4(5)	0.003 0(12)
B(8)	0.310 6(9)	0.194 4(5)	-0.483 6(10)	C(15b)	0.313 3(10)	-0.173 7(5)	-0.128 7(12)
B(9)	0.475 5(10)	0.191 8(5)	-0.508 2(11)	C(13c)	0.061 3(7)	-0.002 5(4)	0.497 5(9)
B(10)	0.552 2(10)	0.222 8(5)	-0.346 7(11)	C(14c)	0.296 7(9)	-0.043 8(5)	0.480 9(10)
B(11)	0.432 9(10)	0.245 0(5)	-0.224 5(11)	C(15c)	0.290 8(9)	0.017 8(5)	0.495 6(10)
B(12)	0.426 8(10)	0.175 9(5)	-0.352 1(11)	C(13d)	0.003 7(9)	0.030 9(4)	-0.007 5(10)
C(16)	0.360 7(8)	0.385 8(4)	-0.436 0(9)	C(14d)	0.020 1(10)	0.150 1(5)	0.037 1(11)
C(17)	0.342 6(8)	0.443 4(4)	-0.330 2(8)	C(15d)	0.011 3(10)	0.131 0(5)	-0.097 6(12)
C(18)	0.331 1(10)	0.496 5(5)	-0.394 1(11)	C(13e)	0.527 3(9)	0.472 7(4)	0.013 6(10)
C(19)	0.346 7(9)	0.482 5(5)	-0.528 4(11)	C(14e)	0.577 6(12)	0.366 7(6)	0.098 3(13)
C(1a)	0.020 1(8)	0.334 4(4)	-0.346 5(8)	C(15e)	0.682 5(12)	0.375 5(6)	0.055 3(13)

Table 6 Fractional atomic coordinates for complex 3

Atom	x	y	z	Atom	x	y	z
S(1a)	-0.0014(6)	0.0076(2)	0.2197(5)	S(20)	0.5612(10)	-0.1140(3)	0.7037(9)
S(2a)	0.2442(6)	-0.0163(2)	0.1682(5)	S(20')	0.8024(16)	-0.1577(7)	0.7208(15)
S(1b)	-0.0476(7)	0.0845(2)	0.0434(6)	C(17)	0.7785(41)	-0.1616(23)	0.7363(40)
S(2b)	0.1938(7)	0.0593(2)	-0.0142(6)	C(17')	0.5612(10)	-0.1140(3)	0.7037(9)
Fe(3)	0.5479(3)	-0.1414(1)	0.3843(3)	C(19)	0.6235(22)	-0.1431(8)	0.8154(20)
C(14a)	0.0925(20)	-0.0332(7)	0.2942(18)	C(18)	0.7315(23)	-0.1644(8)	0.8245(21)
C(15a)	0.2025(21)	-0.0435(7)	0.2680(18)	C(16)	0.6890(20)	-0.1260(6)	0.6463(18)
C(13a)	0.1037(18)	0.0173(6)	0.1431(16)	C(1)	0.6828(19)	-0.1059(6)	0.5320(17)
C(13b)	0.0905(19)	0.0497(6)	0.0657(17)	B(4)	0.5430(22)	-0.0792(8)	0.4480(20)
C(14b)	-0.0077(22)	0.1140(7)	-0.0593(19)	B(8)	0.5501(23)	-0.0818(8)	0.2998(21)
C(15b)	0.1022(22)	0.1027(7)	-0.0814(20)	B(7)	0.6964(25)	-0.1178(9)	0.3063(23)
C(16a)	0.7016(20)	-0.2252(6)	0.4209(18)	C(2)	0.7686(19)	-0.1297(6)	0.4616(16)
C(17a)	0.7734(17)	-0.2407(5)	0.5303(15)	B(6)	0.8471(24)	-0.0870(8)	0.5488(22)
C(18a)	0.9100(22)	-0.2499(8)	0.5333(21)	B(5)	0.7005(24)	-0.0523(8)	0.5404(22)
C(19a)	0.9398(20)	-0.2417(7)	0.4399(18)	B(9)	0.6267(23)	-0.0370(8)	0.3911(21)
S(20a)	0.8025(8)	-0.2231(2)	0.3343(7)	B(12)	0.7219(23)	-0.0633(8)	0.3025(21)
C(1a)	0.5519(20)	-0.2083(6)	0.3753(18)	B(11)	0.8526(25)	-0.0924(9)	0.4072(22)
C(2a)	0.4857(19)	-0.1924(6)	0.4744(16)	B(10)	0.8103(26)	-0.0438(9)	0.4496(23)
B(7a)	0.3566(22)	-0.1548(8)	0.4122(20)	C(1s)	-0.2996(12)	0.1390(4)	0.1176(12)
B(8a)	0.3417(23)	-0.1520(8)	0.2619(21)	C(2s)	-0.3805(12)	0.1147(4)	0.0248(12)
B(4a)	0.4807(23)	-0.1847(8)	0.2404(21)	C(3s)	-0.4084(12)	0.0736(4)	0.0438(12)
B(6a)	0.4471(23)	-0.2428(8)	0.4188(21)	C(4s)	-0.3554(12)	0.0567(4)	0.1556(12)
B(11a)	0.3120(25)	-0.2081(9)	0.4404(23)	C(5s)	-0.2745(12)	0.0809(4)	0.2483(12)
B(12a)	0.2165(23)	-0.1841(8)	0.3013(21)	C(6s)	-0.2466(12)	0.1221(4)	0.2293(12)
B(9a)	0.2954(25)	-0.2017(9)	0.1981(22)	C(7s5)	-0.2237(37)	0.0719(16)	0.3696(35)
B(5a)	0.4323(22)	-0.2384(8)	0.2683(20)	C(7s6)	-0.1769(34)	0.1478(15)	0.3179(32)
B(10a)	0.2748(24)	-0.2362(8)	0.3095(22)				

parameters of 0.08 Å² but their positions were not refined. After refinement with isotropic thermal parameters for all atoms, an empirical absorption correction³² was applied (maximum 1.066, minimum 0.798). Individual weights of 1/σ²(*F*) were assigned to each reflection and in the final cycles of full-matrix least-squares refinement the iron and sulfur atoms were given anisotropic thermal parameters; refinement converged at *R* = 0.0575, *R*' = 0.0568 for 299 parameters.

[*ttf*]⁺[Fe(C₂B₉H₁₀C₄H₃S)₂]⁻·C₆H₅Me 3. The position of

the iron atom was obtained from a Patterson synthesis and the non-hydrogen atoms of the carborane cage and the [*ttf*]⁺ cation were located by subsequent Fourier-difference-syntheses. Remaining electron density was assigned to a toluene solvate molecule with its methyl group disordered over two atoms of the ring in a 50:50 ratio. The aromatic ring of the solvate was constrained to refine in an idealised geometry (C-C 1.395 Å, C-C-C 120°). Relatively high and low isotropic thermal parameters were associated with the sulfur atom S(20) and the

opposite carbon atom C(17), respectively, of one thiophene ring of the substituted metallacarborane; these were attributed to a disorder corresponding to a 180° rotation of the ring about the C(1)–C(16) bond which exchanges the carbon and sulfur positions. While the peak nominally labelled C(17) was resolved into two closely spaced maxima corresponding to the carbon and sulfur atoms C(17) and S(20') respectively (occupancy ratio 0.55:0.45), the 'opposite' site in the thiophene ring [labelled S(20) and C(17')] could not be resolved and so was assigned carbon and sulfur occupancies in the ratio 0.45:0.55. This gave satisfactory refinement and was consistent with the rotation disorder model. Hydrogen atoms of the [tff]⁺ cation and non-disordered hydrogens of the toluene solvate were included in idealised positions (C–H 1.08 Å) with fixed isotropic thermal parameters (0.08 and 0.11 Å² respectively). An empirical absorption correction³² was applied (maximum 1.037, minimum 0.948) after refinement with isotropic thermal parameters for all non-hydrogen atoms. Individual weights of 1/σ²(*F*) were assigned to each reflection and in the final cycles of full-matrix least-squares refinement anisotropic thermal parameters were assigned to the iron atom of the metallacarborane and the sulfur atoms of the [tff]⁺ cation. Refinement converged at *R* = 0.0829 and *R'* = 0.0800 for 225 parameters.

Fractional atomic coordinates for compounds **2** and **3** are given in Tables 5 and 6 respectively.

Additional material available from the Cambridge Crystallographic Data Centre comprises H-atom coordinates, thermal parameters and remaining bond lengths and angles.

Acknowledgements

Support of this work by the SERC is acknowledged. Y.-K. Y. thanks the Nanyang Technological University, Singapore, for a scholarship and D. M. P. M. thanks BP for a generous endowment.

References

- J. M. Williams, J. R. Ferraro, R. J. Thorn, K. D. Carlson, U. Geiser, H. H. Wang, A. M. Kini and M.-H. Whangbo, *Organic Superconductors (including Fullerenes): Synthesis, Structure, Properties and Theory*, Prentice Hall, Englewood Cliffs, NJ, 1992; J. A. Schlueter, Y. Orihashi, M. G. Kanatzidis, W. Liang, T. J. Marks, D. C. DeGroot, H. O. Marcy, W. J. McCarthy, C. R. Kannewurf and T. Inabe, *Chem. Mater.*, 1991, **3**, 1013; Y. Misaki, K. Kawakami, T. Matsui, T. Yamabe and M. Shiro, *J. Chem. Soc., Chem. Commun.*, 1994, 459; M. J. Rosseinsky, M. Kurmoo, P. Day, I. R. Marsden, R. H. Friend, D. Chasseau, J. Gaultier, G. Bravic and L. Ducasse, *J. Mater. Chem.*, 1993, **3**, 801; M. Kurmoo, P. Day, A. M. Stringer, J. A. K. Howard, L. Ducasse, F. L. Pratt, J. Singleton and W. Hayes, *J. Mater. Chem.*, 1993, **3**, 1161.
- J. S. Miller, J. C. Calabrese, H. Rommelmann, S. R. Chittipeddi, J. H. Zhang, W. M. Reiff and A. J. Epstein, *J. Am. Chem. Soc.*, 1987, **109**, 769; W. E. Broderick, J. A. Thompson, E. P. Day and B. M. Hoffman, *Science*, 1990, **249**, 401; J. M. Manriquez, G. T. Yee, R. S. McLean, A. J. Epstein and J. S. Miller, *Science*, 1991, **252**, 1415; Y. Pei, O. Kahn, K. Nakatani, E. Codjovi, C. Mathonière and J. Sletten, *J. Am. Chem. Soc.*, 1991, **113**, 6558; V. Gadet, T. Mallah, I. Castro, M. Verdaguier and P. Veillet, *J. Am. Chem. Soc.*, 1992, **114**, 9213; J. S. Miller, R. S. McLean, C. Vazquez, J. C. Calabrese, F. Zuo and A. J. Epstein, *J. Mater. Chem.*, 1993, **3**, 215.
- I. R. Marsden, M. L. Allan, R. H. Friend, M. Kurmoo, D. Kanazawa, P. Day, G. Bravic, D. Chasseau, L. Ducasse and W. Hayes, *Phys. Rev. B*, 1994, **50**, 2118; P. Day, M. Kurmoo, T. Mallah, I. R. Marsden, R. H. Friend, F. L. Pratt, W. Hayes, D. Chasseau, J. Gaultier, G. Bravic and L. Ducasse, *J. Am. Chem. Soc.*, 1992, **114**, 10722; Y. I. Kim and W. E. Hatfield, *Inorg. Chim. Acta*, 1991, **188**, 15; A. Penicaud, P. Batail, C. Perrin, C. Coulon, S. S. P. Parkin and J. B. Torrance, *J. Chem. Soc., Chem. Commun.*, 1987, 330.
- J. M. Forward, D. M. P. Mingos, T. E. Müller, D. J. Williams and Y.-K. Yan, *J. Organomet. Chem.*, 1994, **467**, 207.
- J. M. Williams, H. H. Wang, T. J. Emge, U. Geiser, M. A. Beno, P. C. W. Leung, K. D. Carlson, R. J. Thorn, A. J. Schultz and M.-H. Whangbo, *Prog. Inorg. Chem.*, 1987, **35**, 51.
- G. Saito and J. P. Ferraris, *Bull. Chem. Soc. Jpn.*, 1980, **53**, 2141.
- M. F. Hawthorne, T. D. Andrews, P. M. Garrett, F. P. Olsen, M. Reintjes, F. N. Tebbe, L. F. Warren, P. A. Wegner and D. C. Young, *Inorg. Synth.*, 1967, **10**, 91.
- T. L. Heying, J. W. Ager, jun., S. L. Clark, D. J. Mangold, H. L. Goldstein, M. Hillman, R. J. Polak and J. W. Szymanski, *Inorg. Chem.*, 1963, **2**, 1089; M. M. Fein, J. Bobinski, N. Mayes, N. Schwartz and M. S. Cohen, *Inorg. Chem.*, 1963, **2**, 1111; M. M. Fein, D. Grafstein, J. E. Paustian, J. Bobinski, B. M. Lichstein, N. Mayes, N. N. Schwartz and M. S. Cohen, *Inorg. Chem.*, 1963, **2**, 1115; J. A. Dupont and M. F. Hawthorne, *J. Am. Chem. Soc.*, 1964, **86**, 1643; V. Gregor, S. Hermánek and J. Plešek, *Collect. Czech. Chem. Commun.*, 1968, **33**, 980.
- M. F. Hawthorne, D. C. Young, T. D. Andrews, D. V. Howe, R. L. Pilling, A. D. Pitts, M. Reintjes, L. F. Warren, jun. and P. A. Wegner, *J. Am. Chem. Soc.*, 1968, **90**, 879.
- D. L. Coffen, J. Q. Chambers, D. R. Williams, P. E. Garrett and N. D. Canfield, *J. Am. Chem. Soc.*, 1971, **93**, 2258.
- C. Bellitto, M. Bonamico, V. Fares, P. Imperatori and S. Patrizio, *J. Chem. Soc., Dalton Trans.*, 1989, 719.
- J. S. Kasper, L. V. Interrante and C. A. Secaur, *J. Am. Chem. Soc.*, 1975, **97**, 890.
- K. Kikuchi, K. Yakushi, H. Kuroda, I. Ikemoto, K. Kobayashi, M. Honda, C. Katayama and J. Tanaka, *Chem. Lett.*, 1985, 419.
- S. S. Shaik and M.-H. Whangbo, *Inorg. Chem.*, 1986, **25**, 1201.
- W. F. Cooper, N. C. Kenny, J. W. Edmonds, A. Nagel, F. Wudl and P. Coppens, *Chem. Commun.*, 1971, 889.
- T. J. Kistenmacher, T. E. Phillips and D. O. Cowan, *Acta Crystallogr., Sect. B*, 1974, **30**, 763.
- K. Yakushi, S. Nishimura, T. Sugano, H. Kuroda and I. Ikemoto, *Acta Crystallogr., Sect. B*, 1980, **36**, 358.
- Cambridge Structural Database, Version 5.6, 1994; F. H. Allen, J. E. Davies, J. J. Galloy, O. Johnson, O. Kennard, C. F. Macrae, E. M. Mitchell, G. F. Mitchell, J. M. Smith and D. G. Watson, *J. Chem. Inf. Comput. Sci.*, 1991, **31**, 187.
- K. Nakasuji, M. Nakatsuka, H. Yamochi, I. Murata, S. Harada, N. Kasai, K. Yamamura, J. Tanaka, G. Saito, T. Enoki and H. Inokuchi, *Bull. Chem. Soc. Jpn.*, 1986, **59**, 207.
- A. S. Batsanov, M. R. Bryce, S. R. Davies, J. A. K. Howard, R. Whitehead and B. K. Tanner, *J. Chem. Soc., Perkin Trans. 2*, 1993, 313.
- R. Bozio, I. Zanon, A. Girlando and C. Pecile, *J. Chem. Phys.*, 1979, **71**, 2282.
- J. B. Torrance, B. A. Scott, B. Welber, F. B. Kaufman and P. E. Seiden, *Phys. Rev. B*, 1979, **19**, 730.
- M. J. Rice, V. M. Yartsev and C. S. Jacobsen, *Phys. Rev. B*, 1980, **21**, 3437.
- V. M. Yartsev, *Phys. Status Solidi, Sect. B*, 1984, **126**, 501.
- E. Hernández, M. Mas, E. Molins, C. Rovira and J. Veciana, *Angew. Chem., Int. Ed. Engl.*, 1993, **32**, 882.
- K. Honda, *Ann. Phys. (Leipzig)*, 1910, **32**, 1003; M. Owen, *Ann. Phys. (Leipzig)*, 1912, **37**, 657.
- P. Kovacic and N. O. Brace, *Inorg. Synth.*, 1960, **6**, 172; G. W. A. Fowles, D. A. Rice and R. A. Walton, *J. Inorg. Nucl. Chem.*, 1969, **31**, 3119.
- J.-P. Beny, S. N. Dhawan, J. Kagan and S. Sundlass, *J. Org. Chem.*, 1982, **47**, 2201.
- A. J. Gordon and R. A. Ford, *The Chemist's Companion: A Handbook of Practical Data, Techniques and References*, Wiley-Interscience, New York, 1972.
- M. K. Cooper, P. A. Duckworth, K. Henrick and M. McPartlin, *J. Chem. Soc., Dalton Trans.*, 1981, 2357.
- G. M. Sheldrick, SHELX 76, University of Cambridge, 1976; SHELX 86, University of Göttingen, 1986.
- N. Walker and D. Stuart, *Acta Crystallogr., Sect. A*, 1983, **39**, 158.

Received 9th March 1995; Paper 5/01455G